

## Ultrashort Pulse Laser Microsurgery System with Plasma Luminescence Feedback Control

B.-M. Kim, M. D. Feit, A. M. Rubenchik, D. M. Gold, C. B. Darrow, L. B. Da Silva  
Medical Technology Program, Lawrence Livermore National Laboratory, Livermore, CA, USA

### ABSTRACT

Plasma luminescence spectroscopy was used for precise ablation of bone tissue during ultrashort pulse laser (USPL) micro-spinal surgery. Strong contrast of the luminescence spectra between bone marrow and spinal cord provided the real time feedback control so that only bone tissue can be selectively ablated while preserving the spinal cord.

### INTRODUCTION

As lasers are accepted as possible replacement for conventional surgical tools in many medical fields, a focus of research has been on more effectively removing the malignant tissues while reducing mechanical/thermal damage to the surrounding tissues. Recently, many studies showed that ultrashort pulse lasers ( $< 1$  ps) can meet this need [1] - [6]. In this short pulse domain, the ablation process is distinguished from the conventional longer pulse ablation which mostly depends on the photothermal heating in the media. As the pulse width becomes shorter, multiphoton ionization dominates during the ablation process which leads to the plasma optical breakdown. The plasma is ejected at a rate  $\sim 10^7$  cm/s which is faster than the shockwave speed  $\sim 10^6$  cm/s and the even slower heat diffusion speed. Therefore, the mechanical/thermal damage is minimized with these short pulses. Additionally, since the plasma is highly reflective, for longer pulses such as 1 ns pulses, a large fraction of the incoming energy is reflected back or channeled into plasma heating instead of being absorbed by the tissue and used for tissue removal. On the other hand, the ultrashort pulse is much shorter than the plasma expansion time and therefore the ablation is highly effective ( $\sim 1\mu\text{m}/\text{pulse}$ ) [2]. Figs. 1 and 2 show the ablated craters on tooth and porcine myocardium respectively. The mechanical cracks that are normally seen on tooth with 1 ns pulses are not observed when USPL was used. Similarly, the thermal damage on myocardium which is obvious along the axis of the collagen fibers for longer pulses are minimal in USPL ablated crater.

The luminescence is generated from a high temperature plasma during ablation. The strong luminescence signals for calcium based plaque in atherosclerotic tissue has been reported [7] - [9]. Our studies are focused on the feasibility test of using the luminescence spectroscopy as a tool for optical feedback during micro-spinal surgery where the calcium based bone tissue needs to be removed while preserving the soft nerve tissue which stems from the spinal cord. The results suggest that the hard tissue can be selectively ablated with high accuracy.

### RESULTS AND DISCUSSIONS

Our ultrashort pulse laser ablation system is equipped with four separate lasers. An 82 MHz Ti-Sapphire actively mode-locked laser (Spectra Physics, Model # 3960) is pumped by a 5 W, frequency doubled Nd:YAG laser (Spectra Physics Model : Millenia) running at 532 nm. The mode-locked laser pulse has duration of 100 fs at 790 nm. Its pulse is amplified by a Ti-Sapphire regenerative amplifier (Positive Light, Model : Spitfire) through a chirped pulse amplification (CPA) process. This amplifier is pumped by a 10 W, 527 nm Nd:YLF laser (Positive Light, Model : Merlyn). The final pulse duration is about 150 fs running at 1 kHz and its amplified energy is more than 1 mJ/pulse at 790 nm. The ablation rate is approximately 1 mm/s using a 1 kHz beam train. The focused beam size was less than 150  $\mu\text{m}$  with TEM 00 mode.

A fresh porcine spine was frozen and cut transversely to expose the bone marrow and spinal cord. The cross section was cleaned with a soft brush to remove the debris of the soft tissue left in the bone marrow during cutting. The laser pulses were focused onto the cross sections of spinal cord and bone marrow to generate the plasma luminescence.

In a basic experimental setup, the luminescence signal was collected by a 1 mm diameter optical fiber and was delivered to the spectrometer and charged coupled device (CCD) camera. The source light was normally incident onto the tissue and the fiber was placed 20° from the normal direction and 5 mm away from the tissue surface. A mechanical shutter for the source laser and a CCD shutter were controlled by a pulse generator. Fig. 3 shows the luminescence spectra from both bone and spinal cord. As seen from the figure, not only the overall luminescence intensity is strong but strong calcium lines are observed from the bone luminescence spectrum. On the other hand, the luminescence from the spinal cord is negligible.

The overall luminescence intensity decreases as the ablation front moves deeper into the ablation hole because less ablated material is ejected and the distance between the ablation front and detector becomes larger as discussed in the previous study [10]. From this study, it was concluded that by comparing the luminescence between 616 nm and 575 nm, we can accurately discriminate the two tissue types. The ratios between these two wavelengths (616 nm/575 nm) were 4.8 for bone and 1.4 for spinal cord.

In a more practical setup as shown in Fig. 4, this beam was delivered and focused onto the tissue using an articulated arm which is composed of seven separate high damage threshold mirrors and one focusing lens. The luminescence signal was collected by a 200  $\mu\text{m}$  optical fiber which is attached on the handpiece of the articulated arm and connected to a 1x2 fiber coupler. This signal

was detected by two photomultiplier tubes (PMT) which are equipped with 616 nm and 575 nm bandpass filters respectively. To remove the intense laser source light, an additional short wave pass filter with cut-off wavelength at 650 nm were added to each PMT's providing optical density of 7 for the source light. The typical luminescence signals for these two detectors are shown in Fig. 5. The initial strong peak corresponds to the laser source light which is too strong to be filtered even by the OD 7 filters. Each detected signal was gated and integrated immediately after the strong peak laser signal so that only the secondary luminescence can be collected. The integrated signal was compared in a computer and a TTL signal was generated to determine if the tissue is bone or spinal cord and to control the laser shutter. When the laser hit the spinal cord, the computer send an "off" signal to the mechanical shutter to close it. After the ablation stops, the shutter reopens after a short duration of 0.5 sec so that the surgeon can keep ablating the bone.

Since luminescence spectroscopy requires a small fraction of the tissue to be ablated, it is of concern how to minimize the damage to the soft tissue. As mentioned earlier, the ablation rate for this short pulse width is approximately 1  $\mu\text{m}/\text{pulse}$ . The future goal of the study will focus on limiting the damage to less than 5  $\mu\text{m}$  which is believed to cause negligible damage to nerve tissue. To accomplish this, a fast electronics package is under development. Currently, the possible maximum damage is between 10 - 15  $\mu\text{m}$ .

### CONCLUSION

We demonstrated that a safe and precise microsurgery using ultrashort pulse laser can be performed. The two wavelength comparison technique provides accurate selective tissue ablation.

### REFERENCES

- [1] B. C. Stuart, M. D. Feit, S. Herman, A. M. Rubenchik, B. W. Shore, and M. D. Perry, "Nanosecond-to-femtosecond laser-induced breakdown in dielectrics," *Physical Review*, vol. 53, no. 4, pp. 1749-1761, 1996.
- [2] J. Neev, L. B. Da Silva, M. D. Feit, M. D. Perry, A. M. Rubenchik, and B. C. Stuart, "Ultrashort pulse lasers for hard tissue ablation," *IEEE J. Selected Topics in Quantum Electronics*, vol. 2, no. 4, pp. 790-800, 1996.
- [3] A. A. Oraevsky, L. B. Da Silva, A. M. Rubenchik, M. D. Feit, M. E. Glinsky, M. D. Perry, B. M. Mammini, W. Small, and B. C. Stuart, "Plasma mediated ablation of biological tissues with nanosecond-to-femtosecond laser pulses: Relative role of linear and nonlinear absorption," *IEEE J. Selected Topics in Quantum Electronics*, vol. 2, no. 4, pp. 801-809, 1996.
- [4] L. B. Da Silva, B. C. Stuart, P. M. Celliers, T. D. Chang, M. D. Feit, M. E. Glinsky, N. J. Heredia, S. Herman, S. M. Lane, R. A. London, D. L. Matthews, J. Neev, M. D. Perry, and A. M. Rubenchik, "Comparison of soft and hard tissue ablation with sub-ps and ns pulse lasers," *SPIE Proceedings*, vol. 2681, pp. 196-200, 1996.
- [5] M. D. Feit, A. M. Rubenchik, B.-M. Kim, L. B. Da Silva, and M. D. Perry, "Physical characterization of ultrashort laser pulse drilling of biological tissue," *Applied Surface Science*, 1997, (*in press*)
- [6] R. Birngruber, C. A. Puloafito, A. Gawande, W.-Z. Lin, R. T. Schoenlein, and J. G. Fujimoto, "Femtosecond laser-tissue interaction: Retinal injury studies," *IEEE J. Quantum Electronics*, vol. QE-23, no. 10, pp. 1836-1844, 1987.
- [7] A. A. Oraevsky, S. L. Jacques, G. H. Pettit, F. K. Tittle, and P. D. Henry, "XeCl laser ablation of atherosclerotic aorta," *Lasers Surg. Med.*, vol. 13, pp. 168-178, 1993.
- [8] L. I. Deckelbaum, J. J. Scott, M. L. Stetz, K. M. O'Brien, and G. Backer, "Detection of calcified atherosclerotic plaque by laser-induced plasma emission," *Lasers Surg. Med.*, vol. 12, pp. 18-24, 1992.
- [9] A. A. Oraevsky, R. O. Esenaliev, and V. S. Letokhov, "Temporal characteristics and mechanism of atherosclerotic tissue ablation by nanosecond and picosecond laser pulses," *Lasers in the Life Sciences*, vol. 5, pp. 75-93, 1992.
- [10] B.-M. Kim, M. D. Feit, A. M. Rubenchik, B. M. Mammini, and L. B. Da Silva, "Optical feedback signal for ultrashort laser pulse ablation of tissue," *Applied Surface Science*, 1997 (*in press*)

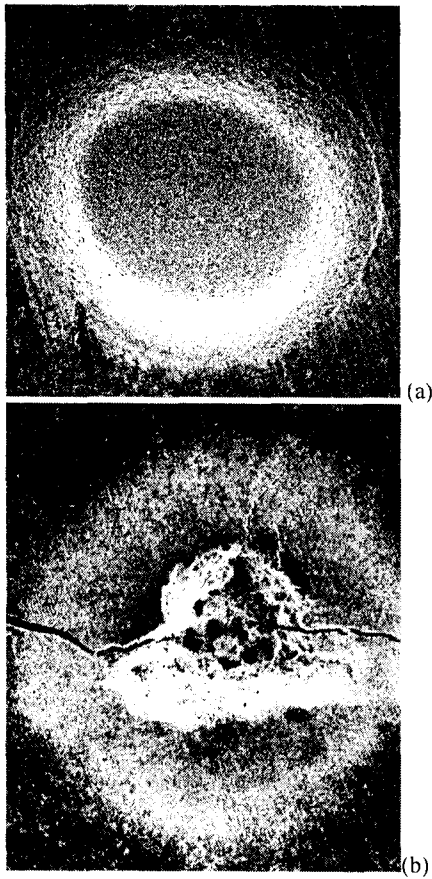


Fig. 1. Ablation craters obtained using (a) 300 fs (USPL), 3 J/cm<sup>2</sup> pulses and (b) 1 ns, 35 J/cm<sup>2</sup> pulses. The mechanical cracks are obvious with longer pulses.

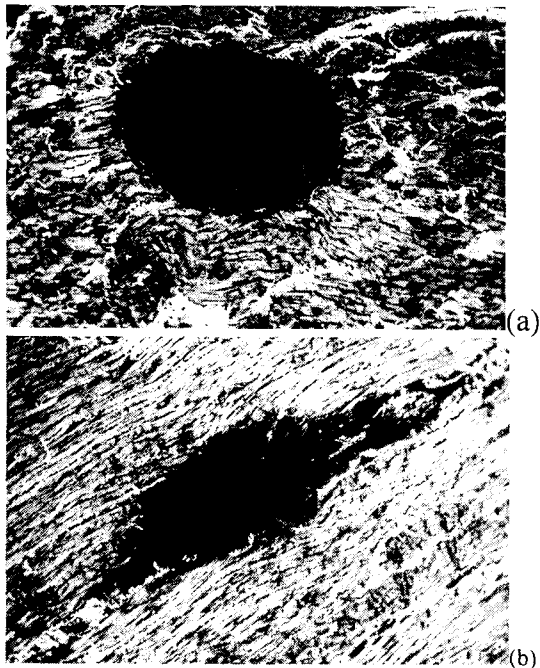


Fig. 2. Holes drilled on pig myocardium using the same parameters as in Fig. 1. USPL crater does not have extensive thermal damage zone.

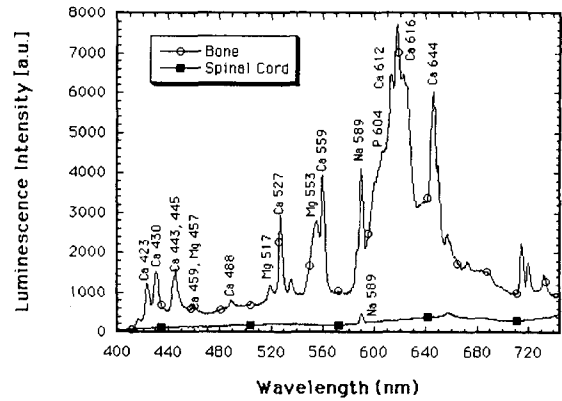


Fig. 3. Luminescence spectra from both porcine bone marrow and spinal cord. Strong calcium lines are observed from the bone spectrum.

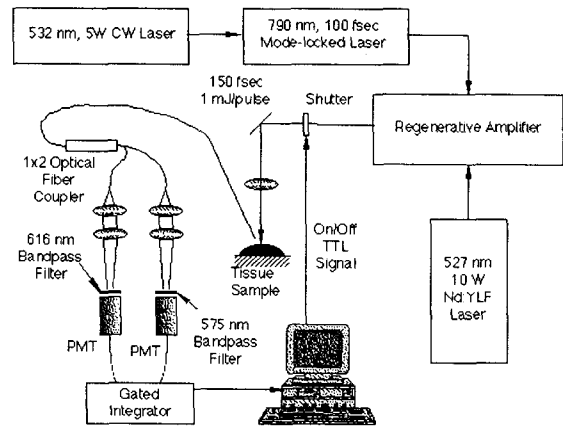


Fig. 4. A schematic for micro-spinal surgery using luminescence feedback control.

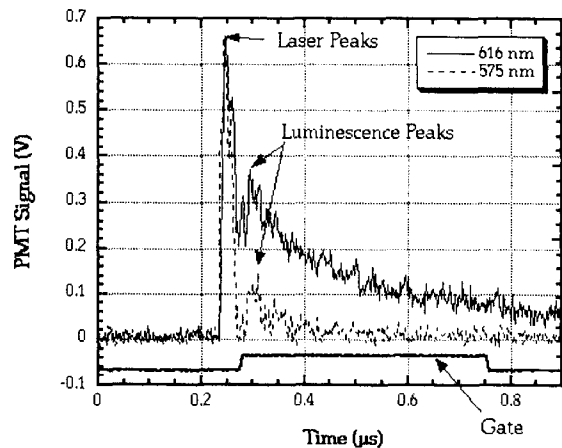


Fig. 5. Typical bone luminescence at 616 nm and 575 nm. Initial strong peak represents the laser source light reflection.